Control of Flowering and Factors Affecting Phenology of Endemic Low-Elevation Tree Species at Hawai'i Ka'ūpūlehu[1]

Thomas Cole[2] and Susan Cordell[2,3]

Abstract: Native dry forest habitat is one of the most threatened and rare ecosystems in the Hawaiian Islands. The Ka'ūpūlehu Dry Forest Preserve, on the west coast of Hawai'i Island, is one of the few remaining intact examples of this low elevation habitat. To aid restoration efforts, flowering phenology of nine native species was estimated monthly from 2001 to 2007. Some species flowered prolifically, others seldom. Two dioecious tree species are in the survey, one only has female flowering trees, the second has both male and female trees. Each gender is treated as a separate species, making ten study "species." The effects of a number of abiotic factors (precipitation, temperature, photoperiod, and insolation) have on flowering are analyzed. Results indicate that flowering phenology of eight species is highly periodic, often correlating with photoperiodism or insolation. Four species are classified as short-day plants, four as long-day plants, and two as neutral-day plants. Both neutral-day species flowered continuously. Critical day length for flowering was determined for four light-dependent flowering species. The amount of precipitation prior to flowering, termed critical rain lag, was determined for seven species. During a multiyear drought, flowering periodicity was found not to depend on precipitation, rainfall only modified the degree of flowering. Several species had significantly more flowering during drought and ceased flowering during wet years. This analysis offers a unique finding of photoperiod the dominant abiotic driver and precipitation secondary, both combining to regulate flowering of dry forest native species.

Keywords: Ka'ūpūlehu, Hawai'i, phenology, dry forest, flowering, photoperiodism, critical day length, critical rain lag, GAM

HAWAI'I'S LOW-ELEVATION native dry forests are one of the most threatened and rare ecosystems in the Hawaiian Islands; an estimate found only 2% of the precontact forest habitat remains today (DOFAW 2019). However, one excellent example of the habitat can still be found on Hawai'i Island. The Ka'ūpūlehu Dry Forest Preserve on the leeward coast of Hawai'i Island was fenced in the 1950s to exclude ungulates. To this day, it remains one of the best examples of native dry forests in the archipelago. The assemblage of species in this dry forest includes several federally endangered species. Although the dry forest habitat is rare, it remains the home to over 40% of all Hawai'i's native land plants, insects, spiders, snails, birds, and Hawai'i's sole native bat (DOFAW 2019).

The introduction of the Pacific rat (*Rattus exulans*) brought by the Polynesians helped expedite the decline of dry forests due to heavy seed predation rates (Cordell and Sandquist 2008). More recent direct impacts such as grazing, fire, and invasive species, coupled with the loss of birds and insects that once pollinated, aided seed dispersal or scarified the seeds of the dry forest species (Stiles 1978,

[1]Manuscript accepted: 6 February 2025.
[2]Institute of Pacific Islands Forestry (IPIF), USDA Forest Service, PSW Station, 60 Nowelo Street, Hilo, HI 96734, USA.
[3]Corresponding author (email: susan.cordell@usda.gov).

Pacific Science (2025), vol. 79, no. 1:71–96
doi:10.2984/79.1.4
ISSN: 0030-8870; E-ISSN: 1534-6188

Olson and James 1982, Wagner et al. 1990, 1999, Libby 2018, Lawson and Rands 2019, Thuma et al. 2023). These species thrive at Kaʻūpūlehu through various agencies' restoration and protection efforts. To support these efforts, we studied the phenology of several dryland tree species. We investigated how abiotic factors (light, temperature, and precipitation) affect flowering. The biological knowledge regarding the time of flowering for these species should help improve their restoration efforts' efficiency. Our results demonstrating how these native species might fare in the hotter, drier, more erratic climate projected for Hawai'i (EPA 2016, 2024) could be critical for their continued survival.

Under natural conditions, many environmental factors influence flowering periodicity (Lang 1965). Primary factors are highly predictable year after year, including the annual change in day length and the period of winter cold (Garner and Allard 1920, Wada 2003, Bernier and Périlleux 2005). More recently, maximum insolation, which occurs on each equinox near the equator, has been found to trigger the induction of flowering of rubber trees (Yeang 2007*a*,*b*, Calle et al. 2010). Secondary abiotic factors are less predictable and include ambient temperature and water availability. Tertiary factors are unpredictable and include mineral availability and competition for resources. Most often, secondary factors only modify the effects of the primary factors. Plants can adapt to local conditions, and species can alternate between primary and secondary factors under unfavorable conditions (Borchert 2024). Some tropical phenological studies still seem to regard photoperiodism and vernalization as unimportant in the control of flowering in the tropics and subtropics (Ralph and Fancy 1994, Wolf et al. 2017) despite photoperiodism having been demonstrated to be a critical trigger in tropical species phenology (Rivera and Borchert 2001, Rivera et al. 2002, Borchert et al. 2005, Yeang 2007*a*,*b*, Calle et al. 2010, Hart et al. 2011, Borchert 2024).

Meteorological factors have often been found not to drive the observed phenology. Still, tracking the phenology of mature, large tropical trees can be challenging and relate it to photoperiod and insolation levels (Borchert 2024, Borchert et al. 2005, 2015, Klebs 1914). The same phenological methodologies recommended by Borchert (2024) were followed during the Kaʻūpūlehu study; however it lasted >6 years, triple the recommended two-year minimum observation period. Depending on the species, the 49–52 monthly observations permit sound statistical conclusions correlating phenophase to abiotic factors utilizing nonlinear statistical methods.

The study aimed to investigate the phenology of flowering of native dry-land species and to determine how flowering was correlated to precipitation, light, and temperature. Field data are collected for flowering, fruiting, and leaf flush, and this paper only analyses flowering. The Kaʻūpūlehu phenology data is archived with the USDA Forest Service and is available for download (Cordell and Cole 2024).

MATERIALS AND METHODS

Study Site

The Kaʻūpūlehu Dry Forest Preserve is located on the northern flank of Hualalai Mountain on the west coast of Hawai'i Island (Figure 1). The site is just south of the 20th parallel north, at latitude 19.77°N,

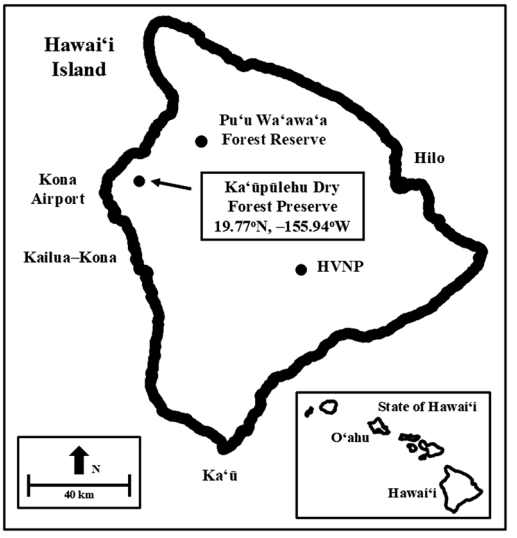

FIGURE 1. Kaʻūpūlehu Dry Forest Preserve, Kaʻūpūlehu, Big Island, State of Hawai'i.

longitude –155.94°W. The Ka‘ūpūlehu Dry Forest Preserve (HFIA 2017) consists of two adjacent parcels of land owned by Kamehameha Schools (http://www.ksbe.edu/). The land is leased to the National Tropical Botanical Garden and PIA Kona Limited Partnership for stewardship. The Mamalahoa Highway (190) bisects the site into a larger northern parcel of 28.4 ha and a smaller southern portion of 2.3 ha. The southern site was fenced by the Territory of Hawai‘i in 1956, and the larger northern site was fenced in 1997. Fencing was intended to prevent ungulates from feeding on the species and protect the habitat from invasive grass species. Fire breaks along the fence lines help protect the site from fire. The average elevation above mean sea level is 630 m. Soils at Ka‘ūpūlehu are 1,500–3,000 years old, extremely rocky, with a‘a lava flows (Moore et al. 1987). Outside the Ka‘ūpūlehu Dry Forest Preserve, the surrounding habitat is heavily invaded by the inflammable nonnative fountain grass, *Pennisetum setaceum* (Cordell and Sandquist 2008). The climate at Ka‘ūpūlehu comprises a hot, dry summer and a wet, stormy winter, a pattern common to leeward coasts of the archipelago (Giambelluca et al. 2013). In 1993, the North Kona Dry Land Forest Working Group (http://www.drylandforest.org/), with numerous partners, including Institute of Pacific Islands Forestry (IPIF) researchers, began restoration efforts at Ka‘ūpūlehu. The institute initiated the present study to aid those efforts.

Field Sampling

The flowering of nine species growing within the Ka‘ūpūlehu Dry Forest Preserve was monitored for 6.3 years, from 20 March 2001 to 6 June 2007 (Appendix 1). Approximately every 1.5 months (46 ± 0.5 days), field ecologists visited Ka‘ūpūlehu and visually estimated flowering density, as a percent of the total crown, of each study tree (Figure 2). In total, there were between 49 and 52 estimates of flowering density for each species, with several (+4) for every month of the year (Table 1). Canopy density visual estimation aids were used by ecologists to also estimate flowering density of our species (Phytosphere 2001). The flowering of 10 trees was monitored for each species, except for the extremely rare *Nothocestrum breviflorum*, which had 4 individuals. To avoid pseudoreplication, the mean of the 10 trees observed during each monitoring visit (observation) was calculated and used in the statistical analysis (Steel and Torrie 1980). The same IPIF forest ecology staff estimated flowering for the entire study.

Species

All nine Ka‘ūpūlehu study trees (Table 1) are endemic to Hawai‘i except for the indigenous *Psydrax odorata*, which is pantropical. Two species are brevideciduous, and the remaining are evergreen. Three species are listed as Endangered by the U.S. Fish and Wildlife Service: *N. breviflorum*, *Dracaena konaensis*, and *Colubrina oppositifolia*. *Pouteria sandwicensis* has been petitioned for listing by the F&W Service (USFWS 2020*a*,*b*). *Nothocestrum breviflorum* is known to have less than 50 individuals left in the wild (USFWS 2020*a*). *Diospyros sandwicensis* and *Xylosma hawaiiensis* are dioecious (male and female flowers on separate trees) (Baker and Cox 1984, Little and Skolmen 1989, Wagner et al. 1990, 1999, Sakai et al. 1995). No male *X. hawaiiensis* trees are in the study, but both sexes of *D. sandwicensis* were included, with each sex treated as a separate species, increasing the number of “species” to 10. The remaining two species were *Santalum paniculatum* (sandalwood) and *Metrosideros polymorpha* var. *polymorpha*, the most culturally important of all Hawaiian native species.

Abiotic Factors

The abiotic factors considered were precipitation, light, and temperature. Nine variables were developed from these abiotic factors. Two variables considered the effects of precipitation, four variables considered the effects of light, and three considered the effects of temperature on flowering phenology. The IPIF operated a weather station onsite from 1999 to 2008 (Figures 3*A*, 3*B*, and 3*C*; Appendices 1.1–1.10). The station collected continuous precipitation, measured in 0.254 mm increments, and recorded air temperature every 10 min. Missing or questionable data were

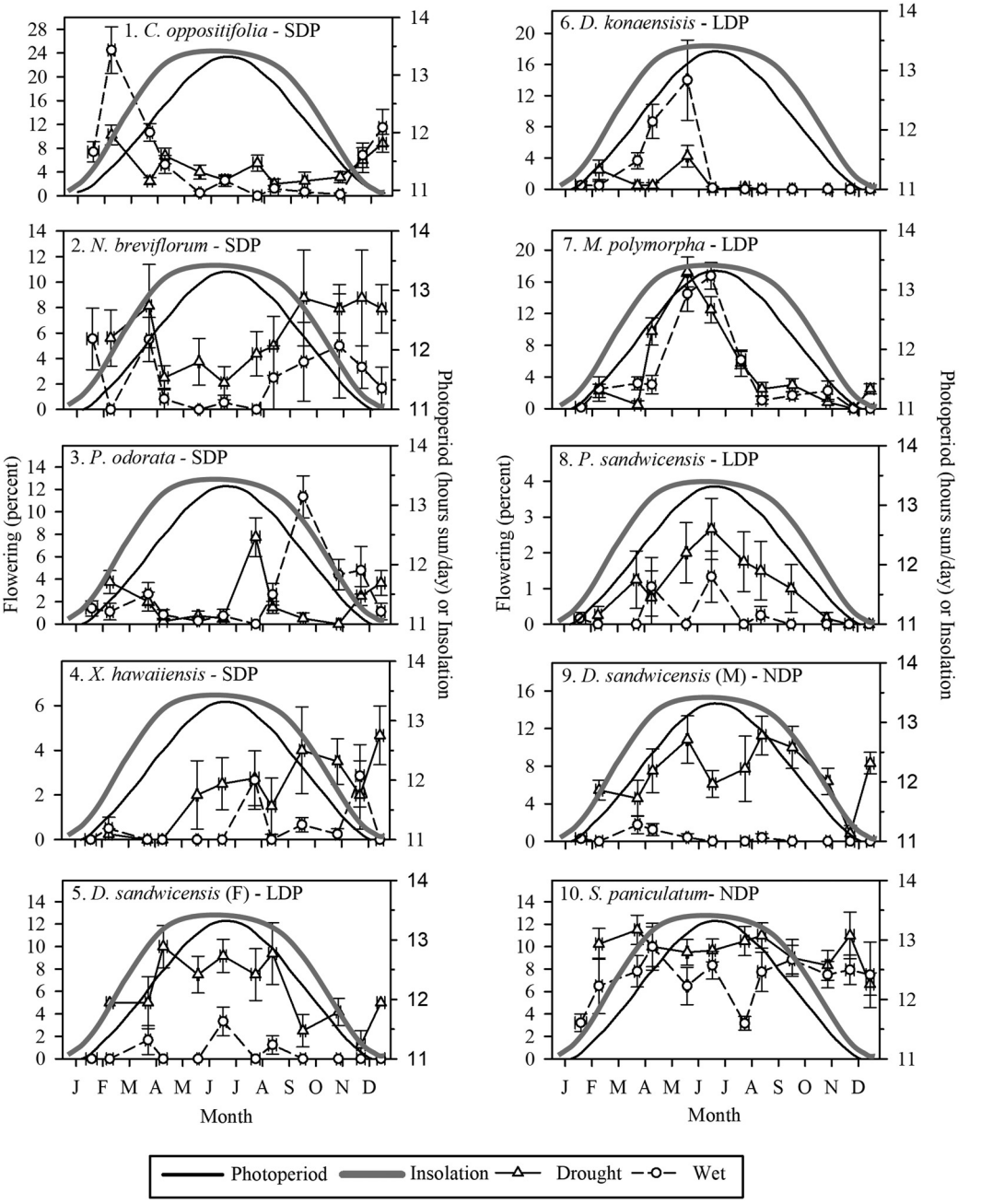

FIGURE 2. Dry land species mean flowering by photoperiodic response type, drought, and annual courses for photoperiod and insolation at 19.8°N latitude. Error bars 95% SE. Kaʻūpūlehu, Hawaiʻi, 2001–2007.

TABLE 1

Scientific and Hawaiian Names for Nine Dry Land Species Growing at the Ka'ūpūlehu Dry Forest Preserve

Scientific Name (Author)	Hawaiian Name	No Tree	No Meas	Status
Colubrina oppositifolia Brongn. ex-Mann	Kauila	10	52	end
Diospyros sandwicensis (A. DC.) Fosberg	Lama	10	52	end
Dracaena konaensisis (H. St. John) Jankalski	Hala pepe	10	52	end
Metrosideros polymorpha Gaud. *var. polymorpha*	'Ōhi'a lehua	10	50	end
Nothocestrum breviflorum A. Gray	'Aiea	4	52	end
Pouteria sandwicensis (A. Gray) Pierre	'Āla'a	10	52	end
Psydrax odorata (G. Forst) A.C. Sm. & S. Darwin	Alahe'e	10	52	ind
Santalum paniculatum Hook. & Arn.	'Iliahi	10	52	end
Xylosma hawaiiensis Seem.	Maua	10	49	end

Shown are the number of trees in the study and number of measurements for each species. Codes are listed below. Ka'ūpūlehu, Hawai'i, 2001–2007.
Rock (1913), Wagner et al. (1990), Sakai et al. (1995), Wagner et al. (1999), Little and Skolmen (1989), and USFWS (2020*a*,*b*).
Codes: Status: ind = indigenous, end = endemic.

replaced with daily measurements from the Ellison Onizuka Kona International Airport NOAA weather station (WRCC 2012), which is approximately 11.5 km west of Ka'ūpūlehu and at 17 m elevation (Figure 1). The climate on the coast is both dryer and hotter than at Ka'ūpūlehu, with the airport receiving about half Ka'ūpūlehu's 500 mm mean annual precipitation.

Daily precipitation was classified into two categories: root-available (total daily precipitation >10 mm) and root-unavailable (total precipitation <10 mm). The soils at Ka'ūpūlehu often develop a crust in dry, hot weather, and exhibit temporary hydrophobic characteristics that prevent absorption until wetting occurs. This moisture, however, tends to evaporate from the soil surface before being absorbed. Only the root-available precipitation was used during the analysis. Removing root-unavailable precipitation reduced annual precipitation by 23%.

The first variable examining rainfall (flowering) must consider the lag between rainfall and each observation. Termed $\text{RainLag}_{\text{days}}$, the variable quantifies the weekly precipitation amount before each observation. RainLag was constructed by summing precipitation weekly for a year prior to each of the 52 observations (RainLag_7, RL_{14}, RL_{21}, . . . , RL_{364}). This was a total of 2,704 rain lag variables for each species. The second precipitation variable analyzes the relationship between extended dry conditions and flowering. Termed DroughtClass, the variable compares flowering during the multiyear drought, 2001–2003, to wetter years, 2004–2007. The DroughtClass variable has a binary data format consisting of two non-integer members. This is important as only integers can be transformed during statistical analysis.

Light's influences on flowering were tested by four variables. The light was quantified as the daytime photoperiod in daylight hours on each observation day (PhotoPer). The daily photoperiod at Ka'ūpūlehu was calculated using a NOAA spreadsheet (Meeus 1999, NOAA 2017). At Ka'ūpūlehu's latitude, 19.8°N, the maximum daytime photoperiod occurs 10 summer days, 16–25 June, with the summer solstice about the midpoint of 20 June. Daytime photoperiod was 13.3 h, and nights were 10.7 h. The 10 days, 16–26 December, with winter solstice about 20 December, had the shortest days (10.9 h) and longest nights (13.1 h). The photoperiod difference between the solstices was thus 2.2 h. An annual plot of photoperiod from the spreadsheet calculator for 2004 was used in the figures.

The second light variable investigated the effects of insolation on flowering. Insolation is the total solar radiation received at a specific

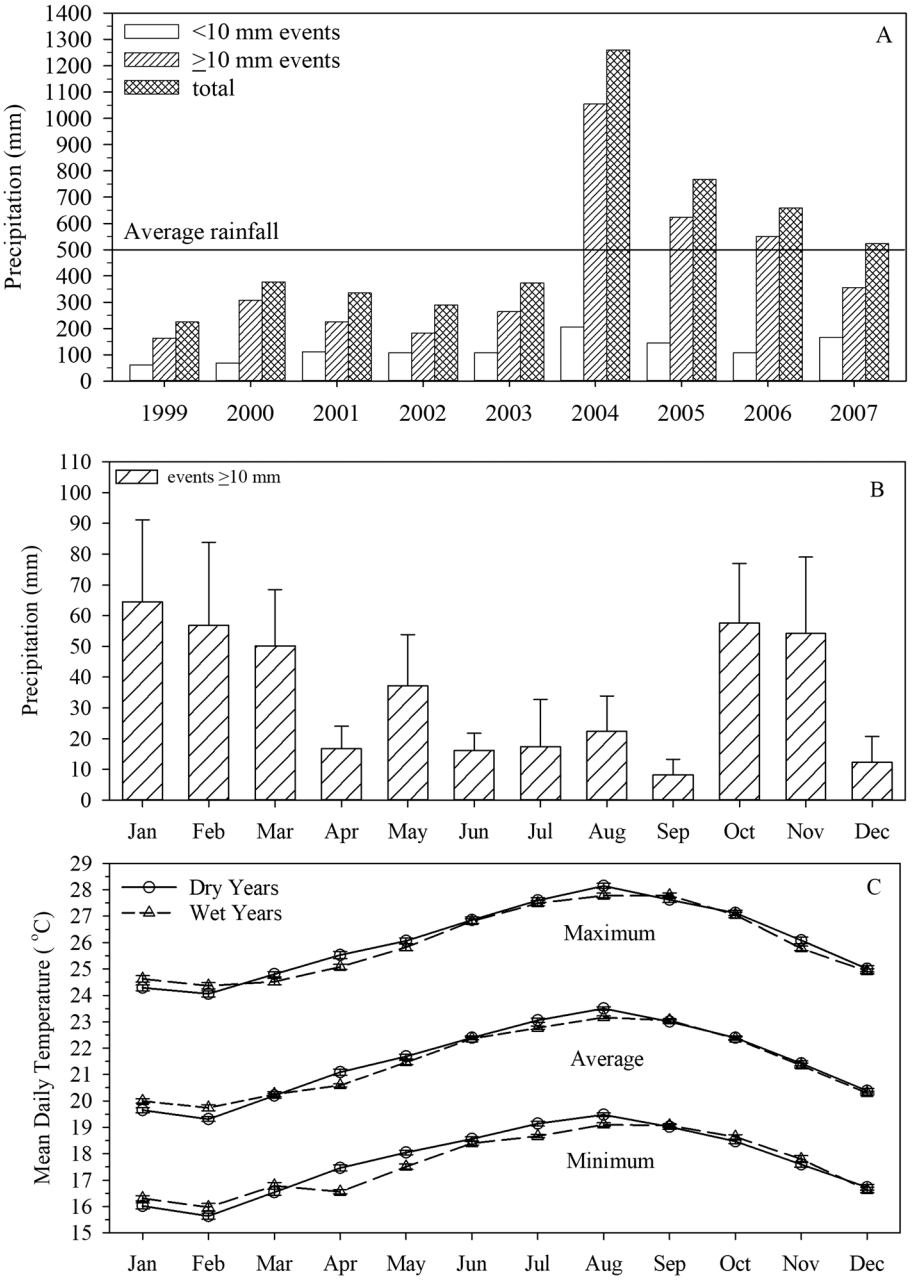

FIGURE 3. Annual precipitation (A), monthly precipitation (B), and monthly air temperature (C). Error bars 95% SE. Kaʻūpūlehu, Hawaiʻi, 1999–2007.

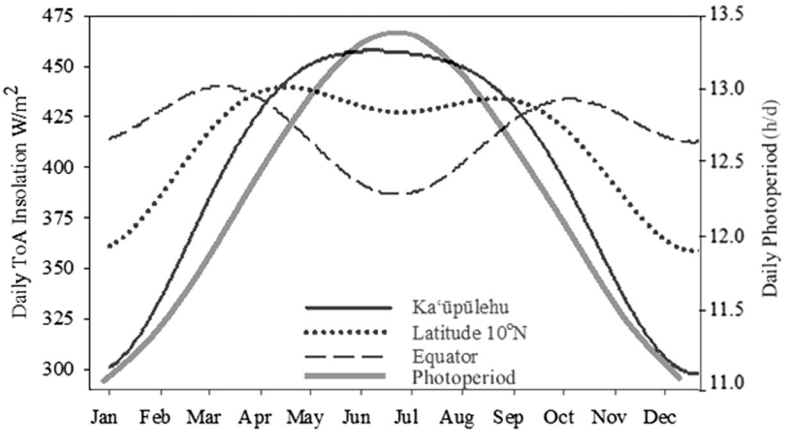

FIGURE 4. Insolation and photoperiod for 2004. Ka'ūpūlehu, Hawai'i, 1999–2007.

latitude (Figure 4). Maximum insolation affected rubber tree flowering near the equator and extending to latitude 22° (Yeang 2007*a*,*b*, Calle et al. 2010). Insolation differs from photoperiod in that insolation considers the reduction in available solar radiation reflected off the top of atmosphere (ToA) and absorbed by atmospheric aerosols, especially clouds. Insolation is, therefore, seasonal following the tilt of the Earth. At Ka'ūpūlehu's latitude (19.77°N), the top of the atmosphere insolation has its maximum (458 W/m^2) three weeks prior (2 June–14 June) to the summer solstice (NASA 2024). The lowest insolation (298 W/m^2) occurs 10 days (15 December–24 December), encompassing the winter solstice. Ka'ūpūlehu has no second peak in maximum insolation nearer the fall equinox, as sites nearer the equator experience. Insolation for 2004 was used in the analysis and figures. Solar radiation striking the ground is estimated to be reduced by 57% by the atmosphere (NASA 2024). Midsummer insolation at Ka'ūpūlehu is 18% greater than at the equator. Maximum insolation at the equator occurs on the equinoxes and averages 5% more than at the study site. Midwinter solar radiation available at Ka'ūpūlehu is 28% lower than at the equator. Annually, Ka'ūpūlehu receives 6% less solar radiation than the equator.

The last two class variables compared flowering phenology during opposite seasons at Ka'ūpūlehu. The first variable, PrecipClass, compared flowering in winter to summer or long to short photoperiods (Borchert 2024). These are also the traditional Hawaiian wet and dry seasons, the timing of which was used to separate the classes. The timing for each class was taken from the Hawaiian moon calendar, with the dry season running from 7 May to 5 November and the wet season from 6 November to 6 May (Hui Mauli Ola 2024). The last variable, PhotoClass, compared flowering fall to spring photoperiods, with the class boundaries being the two solstices or flowering phenology during decreasing or increasing photoperiods (Borchert 2024).

The last three variables are based on the ambient temperatures recorded at Ka'ūpūlehu. The mean annual temperature onsite was 21.6 ± 0.04 °C during the study. The 6.3-year maximum and minimum temperatures recorded during the study were 31.5 °C and 10.6 °C. The three temperature variables are minimum, maximum, and average daily temperature in degrees Celsius. Codes for the variables are MINTc, MAXTc, and AVETc.

Statistical Analyses

Nonlinear generalized additive modeling (GAM) was used in the analysis of flowering (Hastie and Tibshirani 1986, 1990, Efron and Tibshirani 1991, Wood 2006, 2011, Uzoh and Mori 2012, Polansky and Robbins 2013, Wood 2023). GAM modeling can analyze

both nonlinear and linear data, but patterns of flowering are typically nonlinear. The independent variables can be both data types. GAM results are easy to interpret, have flexible predictor functions (that often uncover hidden data patterns), and have the regularization of predictor functions, which helps avoid overfitting. The models have no interaction term (Larsen 2015). In contrast to generalized linear modeling (GLM), the predictor functions from the GAM analysis are additive and easily interpreted. GAM models have been used to analyze flowering responses to temperature and precipitation (Hudson et al. 2003, 2009, Roberts 2008, Gaira et al. 2011).

GAM analyses were performed with R Statistical Software (R Core Team 2023), utilizing the "mgcv" software package. Two functions are run, "gam" and "summary" (Appendix 2; Wood 2023). The analysis performs a mixed GAM analysis with automatic smoothness. The default GAM analysis assumes a Gaussian or two-tailed distribution. The basic GAM statistics include standard errors, *t*-values or *F*-values, and probability levels for each parameter. The goodness of fit statistics are adjusted coefficient of determination (adj. R^2) and unadjusted correlation coefficient (r). The partial residual graphs for each variable are predictive and are the standard graphical output.

GAM Models

GAM selection was done stepwise, working through different combinations of variables and evaluating the contribution or removal of each to the final model (Steel and Torrie 1980). Four models were tested during the GAM selection process, differing only in which variables received transformation. Transforming (ln) flowering data addressed the data's non-normality and nonlinearity and often improved model fit. GAM spline smoothing was done on continuous variables and also often improved model fit and simplified the predictive functions, making their interpretation easier. PhotoPer, INSO, and RainLag were often spline transformed. Class variables cannot be spline transformed. The four models tested were:

$$\text{(a) GAM: flowering} = \text{continuous variables} + \text{class variables}, \quad (1)$$

$$\text{(b) GAM: flowering} = \text{spline(continuous variables)} + \text{class variables}, \quad (2)$$

$$\text{(c) GAM: ln(flowering)} = \text{continuous variables} + \text{class variables}, \quad (3)$$

$$\text{(d) GAM: ln(flowering)} = \text{spline(continuous variables)} + \text{class variables}. \quad (4)$$

Partial residuals graphs are the observed values plotted against the fitted values for each predictive function, plus the residuals from the additive GAM model. The partial residual graphs permit visual evaluation of each variable's effect on flowering. Each variable in the model has an individual partial residual graph, but the effects of each are independent and in total can be discussed additively. Significant levels are $P \leq .05$, and the 95% CI is indicated.

The concept of a critical day length (CDL) important to flowering phenology was first documented over 100 years ago (Garner and Allard 1920, Wada 2003). The GAM analysis identified CDLs for four species (1 SDP and 3 LDP species). CDL was estimated for the other four species as the photoperiod when flowering reached ≥1%. CDL was investigated using the partial residual graphs. CDL was the point where the prediction crosses the origin. At this point, prediction effects switch between negative and positive. Arrows dropped to the *x*-axis indicate the CDL.

A second light critical inflection point was found when total insolation (ToA) affected flowering phenology. Termed critical daily insolation (CDI) and was when the partial residual prediction crosses the origin. Insolation was found to be very sensitive to the timing of maximum flowering; only two species had insolation significance, and both also had

photoperiod significance. The critical inflection points are identified for 1 SDP and 1 LDP species. Each had daily insolation identical (±400 W/m^2) but with opposite slopes of their predictions. CDI was estimated for the remaining six species (SDP *C. oppositifolia*, *P. odorata*, *X. hawaiiensis*; and LDP female *D. sandwicensis* (female), *Dracaena konaensisis*, and *P. sandwicensis*) as the insolation when flowering reached ≥1%. Mean insolation for the 4 SDP species was ≤390 ± 3.5 W/m^2 and for the 4 LDP species ≥405 W/m^2, mean 398 ± 8.1 W/m^2. On the GAM partial residual plots, the slope of insolation is reversed.

The partial residual figure for the precipitation also identified a third critical inflection point, this time for rainfall. Critical rain lag ($RainLag_{days}$ = XX mm rainfall) was where the partial residual function crossed the origin; arrows to the *x*-axis indicate the amount of rainfall. $RainLag_{364}$ = 500 mm is the average annual rainfall at Ka‘ūpūlehu.

RESULTS

Early in assessing the data, the authors could classify all ten species as their flowering response to photoperiod. More recently, insolation has been reported to affect flowering phenology in the tropics (Yeang 2007*a*,*b*, Calle et al. 2010). Each species was classified into one of three biological photosensitive response types: long-day plants (LDP), short-day plants (SDP), or neutral-day plants (NDP), depending on the timing and duration of their flowering (Garner and Allard, 1920). The presentation of the results below is ordered by response type and then alphabetically by species.

The partial residuals graphs are in Figures 5.1–5.10, and Appendix 3 has the model statistics. Mean flowering was calculated from data in Figures 2.1–2.10. A summary of the abiotic effects that influence flowering is in Table 2. Please note that the predictions of insolation on the partial residuals figures have been reversed (Figures 5.2 and 5.7). The figures are labeled to show when maximum flowering occurs.

Short-Day Plants

As is found with all SDP, *C. oppositifolia*’s maximum flowering occurs during the winter (Figure 2.1, Table 2). Flowering appears to be irrespective of drought, and similar flowering patterns are found in dry or wet years. A wet spring does enhance flowering. The flowering of *C. oppositifolia* was 5.0 ± 0.7% by observation (*n* = 52). Two abiotic factors are significant in the GAM analysis, which showed increased flowering with short photoperiods (PrecipClass) and wet conditions, RainLag (R^2 = 48.1, Appendix 3). Winter is also the Hawaiian wet season. The partial residuals had critical rain lag (CRL_{42} ≥ 0 mm) or any precipitation prior to the observation of increased flowering. Photoperiod and insolation are both estimated, CDL was <12.0 h and CDI was <390 W/m^2 when conditions favor *C. oppositifolia* flowering (Figure 5.1).

Nothocestrum breviflorum’s maximum winter flowering periodicity appeared irrespective of drought (Figure 2.2, Table 2). Wet-year flowering still followed the summer/winter pattern, but there was no summer flowering during wet years. *Nothocestrum breviflorum* flowering was mean 4.1 ± 0.5% by observation (*n* = 52). The GAM model showed increased flowering with short photoperiods (PhotoPer), low insolation (INSO), and low precipitation or RainLag (R^2 = 49.8, Appendix 3). CDL was ≤12.2 h and CDI was ≤400 W/m^2 (Figure 5.2). *Nothocestrum breviflorum* flowering followed insolation patterns seen nearer the equator, with two flowering peaks, each on an equinox when maximum insolation occurs (Figure 4). Critical rain lag indicated that dry conditions (CRL_{189} ≤ 285 mm) favor *N. breviflorum* flowering (Figure 5.2).

Maximum *P. odorata* flowering occurred in the fall. Winter and spring flowering was lower and midsummer flowering was almost zero (Figure 2.3, Table 2). Mean *P. odorata* flowering was 2.5 ± 0.6% by observation (*n* = 52). Flowering appeared to be irrespective of drought. Both wet and dry years had similar patterns, but wet year flowering peaked later. The GAM model showed fall’s decreasing photoperiods (PhotoClass) and increased

TABLE 2

Summary of Environmental Factors That Influence the Flowering of Dry Land Species, By Photoperiodic Response Type (PRT)

PRT/Species	Primary Factor	Secondary Factors (SF)	SF Effects	Flowering Season
SDP				
C. oppositifolia	PrC_{winter}↑	$CRL_{42} \geq 0$↑	Wet↑	F/W/SP↑
	≈CDL < 12.0			SU little
	≈CDI < 390			
N. breviflorum	PP ↑↓	$CRL_{189} \leq 285$↑	Dry↑	F/W/SP↑
	CDL ≤ 12.2			SU little
	CDI ≤ 400			Dry W↑
P. odorata	PC_{fall}↑	$CRL_{56} \geq 60$↑	Wet delay	F only
	≈CDL < 12.0		2 mo	SP/SU little
	≈CDI < 390			
X. hawaiiensis	PC_{fall}↑	$DC_{drought}$↑	Dry↑	SU/F/W
	≈CDL<12.0			SP none
	≈CDI<380			
LDP				
D. sandwicensis (female)	PP↑↓	$DC_{drought}$↑	Dry↑	SU
	CDL ≥ 12.4	$CRL_{70} \geq 260$↑	Wet↓	Wet none
	≈CDI > 410			
D. konaensisis	PC_{spring}↑	$CRL_{147} \geq 340$↑	Wet↑	SP/S only
	≈CDL > 12.3		Dry↓	F/W none
	≈CDI > 415			
M. polymorpha	PP↑↓	–	Wet delay 1 mo	SU only
	CDL ≥ 12.3			SP/S/W little
	CDI ≥ 400			
	PC_{spring}↑			
	PrC_{summer}↑			
P. sandwicensis	PP↑↓	$CRL_{217} \leq 250$↑	Dry↑	SU only
	CDL ≥ 12.2			W none
	≈CDI > 400			
	PC_{spring}↑			
NDP				
D. sandwicensis (male)	–	$DC_{drought}$↑	Dry↑	Yr dry
		$CRL_{91} \geq 130$↑		Wet none
S. paniculatum	–	$DC_{drought}$↑	Dry↑	Yr
		MINTc↑	Warmer↑	Wet less

References and codes are below. Ka'ūpūlehu, Hawai'i, 2001–2007.

a. Photoperiodic Response Types: short-day plants (SDP), long-day plants (LDP), and neutral-day plants (NDP).

b. Factors: PhotoPeriod (PP) in hours sunlight/day; Insolation (INSO) = mean 24 hour daily solar radiation at top atmosphere in $W/m^2/d$ (range 298–458 $W/m^2/d$); PhotoClass (PC) = spring/increasing or fall/decreasing photoperiods; PrecipClass (PrC) = summer or winter photoperiod/seasons; DroughtClass (DC) = drought or wet years; $RLAG_{days}$ = rain lag (mm); and MINTc = minimum temperature (degrees Celsius).

c. Flowering inflection points: critical daily insolation (CDI) = daily insolation top atmosphere ($W/m^2/d$); critical daylength (CDL) = hours sunlight/d; and critical rainlag (CRL_{DAYS}) = sum of precipitation over a fixed time period (mm/d). An approximate symbol (≈) indicates that CDL and CDI are estimated.

d. Seasons: summer (SU), fall (F), winter (W), spring (SP), and year-round (Yr).

e. Insolation prediction is reversed from GAM partial residual results in Figure 4.

SDP

1. *Colubrina oppositifolia*

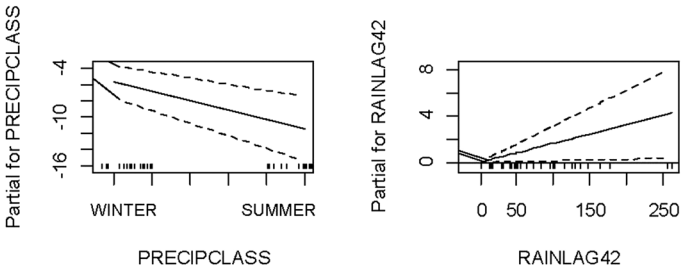

2. *Nothocestrum breviflorum*

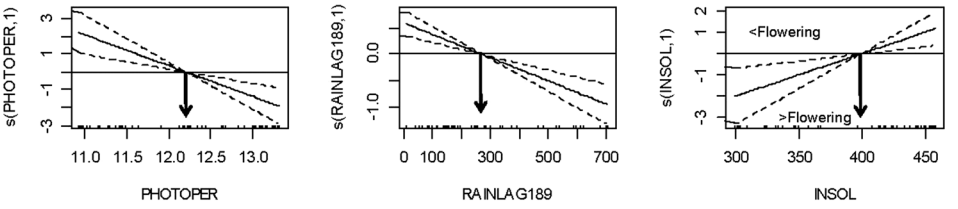

3. *Psydrax odorata*

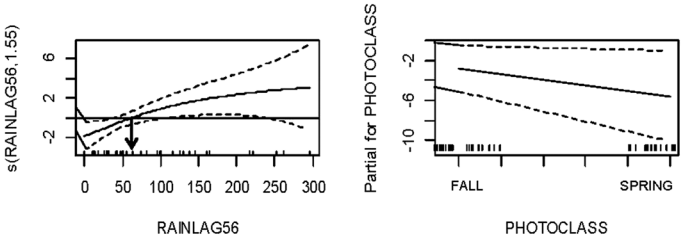

4. *Xylosma hawaiiensis*

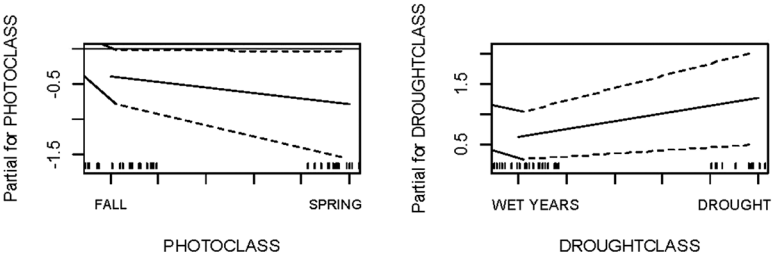

FIGURE 5. Dry land flowering species generalized additive model (GAM) partial residuals. Arrows indicate flowering critical inflection points for photoperiod, insolation, and precipitation. Solid lines are model predictions, dashed lines 95% CI. Codes are below.[1] Ka'ūpūlehu, Hawai'i, 2001–2007.

LDP

5. *Diospyros sandwicensis* (female)

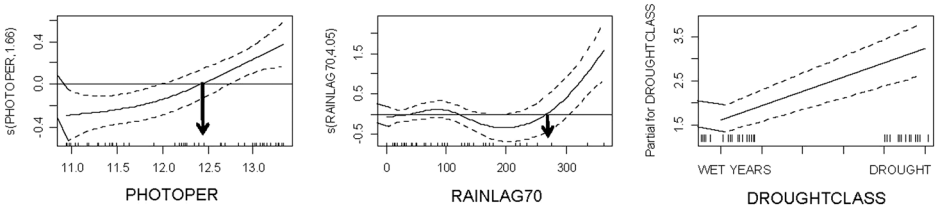

6. *Dracaena konaensisis*

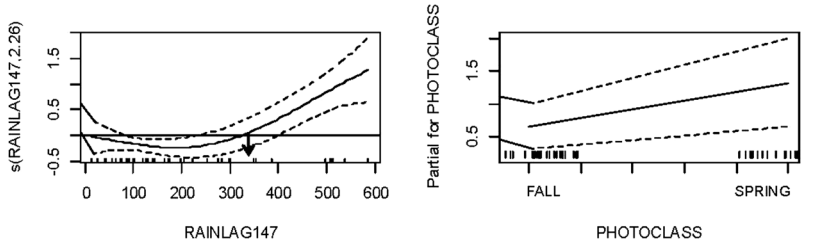

7. *Metrosideros polymorpha*

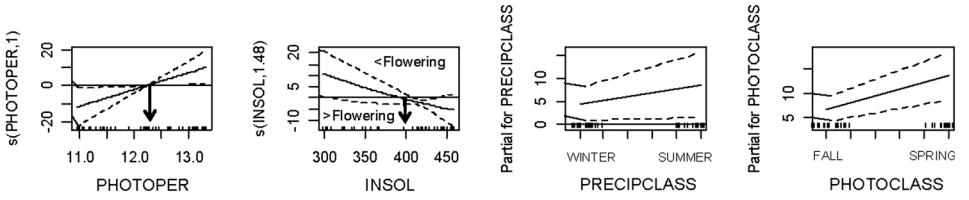

8. *Pouteria sandwicensis*

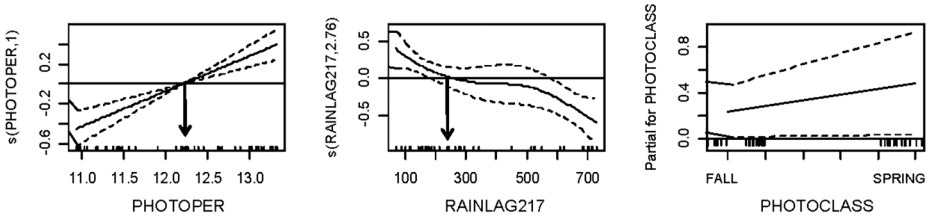

FIGURE 5. (Continued)

precipitation prior to the observation (RainLag) having a positive effect on flowering (R^2 = 15.6%, Appendix 3). Photoperiod and insolation are both estimated, CDL was <12.0 h, critical insolation was <390 W/m^2, and wet critical rain lag (RainLag$_{56}$ ≥ 60 mm) when conditions favor *P. odorata* flowering (Figure 5.3).

NDP

9. *Diospyros sandwicensis* (male)

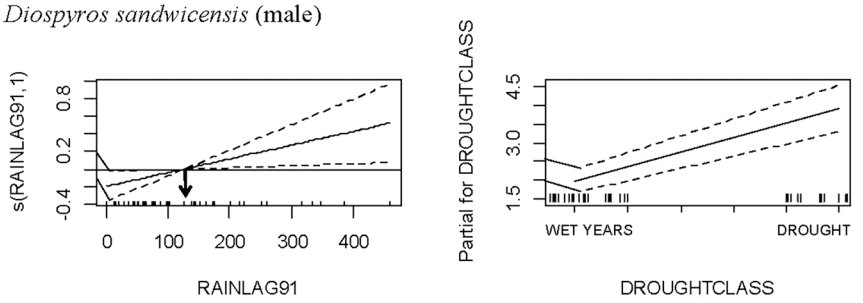

10. *Santalum paniculatum*

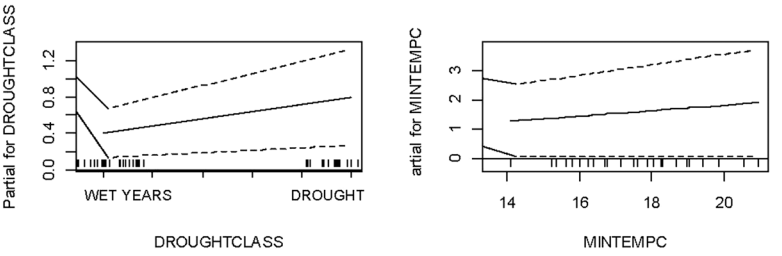

[1]a. Y–axis: Partial = partial residuals, s = spline transformed independent variable.

b. X–axis: DroughtClass = drought/wet years; PHOTOCLASS = spring/fall photoperiod; PrecipClass = summer(dry)/winter(wet) photoperiod/seasons; PhotoPer = photoperiod (h/d; INSO = mean insolation over 24–day (mean W/m^2/d, maximum <450 W/m^2/d); MINTEMPC = minimum daily temperature (^{o}C); and RLAG$_{days}$ = rainlag or sum of precipitation (mm)/days prior measurement (RLAG$_{days}$ = precip.).

c. Graphs for insolation are opposite, more flowering found in negative portion of Y–axis. Reverses greater/less than symbols for insolation in Table 2.

d. Arrows indicate critical inflection points for daylength (CDL), daily insolation (CDI), and rainlag (CRL).

FIGURE 5. (Continued).

Xylosma hawaiiensis's flowering occurred primarily in the late summer and fall, and spring flowering was heavily suppressed (Figure 2.4, Table 2). Flowering periodicity was unchanged by drought, but trees flowered more during dry years. *Xylosma hawaiiensis* average flowering was very low, 1.4 ± 0.4% by observation (n = 49), but occasionally reached 4–5% of the crown. The GAM model shows increased flowering during drought years (DroughtClass) and fall photoperiods, PhotoClass (R^2 = 23.6%, Appendix 3). Photoperiod and insolation are estimated at <12.0 h, with CDI at <380 W/m^2 when conditions favor *X. hawaiiensis* flowering (Figure 5.4).

Long-Day Plants

Female *D. sandwicensis* is the first of the LDP and typical of the response type, has a summer-centric flowering pattern (Figure 2.5,

Table 2). *Diospyros sandwicensis* flowering periodicity was irrespective of precipitation, but drought year flowering was prolific and wet year flowering completely ceased except for some midsummer. Mean flowering was 3.2 ± 0.5% by observation (n = 52). The GAM model indicated long photoperiods (PhotoPer), drought (DroughtClass), and wet RainLag's significantly increasing flowering (R^2 = 80.3%, Appendix 3). The significance of both wet rain lag and drought flowering appear contradictory. The significant rain lag indicated heavy precipitation in the months prior to the observation increased flowering. This precipitation occurred once during the study, January 2004, and is labeled "drought broke" in Appendix 1.2. This was not seen as a positive response to the rainfall, but the last of the drought year had higher flowering. The next observation, flowering, had stopped. CDL was ≥12.4 h, daily insolation was estimated as >410 W/m^2, and critical rain lag ($CRL_{70} \geq 260$ mm), conditions that favor *D. sandwicensis* flowering (Figure 5.5).

Dracaena konaensisis flowered only in the spring and completely stopped flowering just prior to the summer solstice, timing seen in drought and wet years (Figure 2.6, Table 2). Wet-year flowering was 4× greater than drought-year flowering. Large flowering pulses were often seen after heavy spring rains (Appendix 1.4). However, the numerous months with no flowering resulted in a low mean, 1.5 ± 0.6% by observation (n = 52). However, flowering often reached >14% of the crown when in full bloom. The GAM model had spring photoperiods (PhotoClass) and wet RainLag significant (R^2 = 48.9%, Appendix 3). Photoperiod and insolation are estimated, with the CDL being >12.3 h and the insolation being >415 W/m^2. Rain lag ($CRL_{147} \geq 340$) indicated wet conditions favor *D. konaensisis* flowering (Figure 5.6).

Metrosideros polymorpha flowering periodicity followed the LDP pattern and was identical to the bell-shaped curves of photoperiod and insolation (Figure 2.7, Table 2). Precipitation appeared to not affect *M. polymorpha* flowering other than drought flowering occurring a month earlier than during wet years. Mean flowering was 4.9 ± 0.8% by observation (n = 50), and maximum flowering was >16%. The GAM model for *M. polymorpha* has all four light-variables significant. Long photoperiods (PhotoPer), high insolation (INSO), summer photoperiods (PrecipClass), and spring photoperiods (PhotoClass) are all correlated with flowering (R^2 = 66.7%, Appendix 3). PrecipClass is also the dry Hawaiian season. Inflection points for CDL are from each's partial residual figures, CDL ≥ 12.3 h and CDI ≥400 W/m^2 when conditions favor *M. polymorpha* flowering (Figure 5.7).

The *P. sandwicensis* LDP flowering pattern also perfectly matched the photoperiod bell curve (Figure 2.8, Table 2). Drought conditions did not alter flowering periodicity, but wet-year flowering was considerably less than in drought years. Overall, *P. sandwicensis* flowering was very low, only 0.6 ± 0.2% by observation (n = 52). Dry summers do, however, often see >2.0% flowering. The GAM model has long photoperiods (PhotoPer), increasing spring photoperiods (PhotoClass), and dry RainLag significant (R^2 = 44.6%, Appendix 3). CDL was ≥12.2 h, CDI was estimated at >400 W/m^2, and dry critical rain lag ($CRL_{217} \leq 245$ mm) when conditions favor *P. sandwicensis* flowering (Figure 5.8).

Neutral–Day Plants

Classified as NDP, neither photoperiod nor insolation appears to affect male *D. sandwicensis* flowering, which occurred year-round (Figure 2.9, Table 2). Precipitation also did not affect flowering periodicity, but similar to the female trees, there was little flowering during wet conditions. Male flowering *D. sandwicensis* trees have a mean of 3.5 ± 0.6% by observation (n = 52). The GAM model showed wet RainLag and drought (DroughtClass) highly correlated to flowering (R^2 = 78.0%, Appendix 3). As with the female trees, these results are contradictory. The GAM model identified the wet $CRL_{91} \geq 130$ mm when precipitation increases flowering. This amount of precipitation fell once during the study, January 2004. Just after, wet conditions again suppressed flowering (Appendix 1.3). The male trees exhibited no photoperiodic control of flowering and no

CDL or CDI inflection points were identified (Figure 5.9)

Santalum paniculatum flowered throughout the year at Ka'ūpūlehu (Figure 2.10, Table 2) and was the most prolific flowering, dry land species. Flowering appeared to be irrespective of light or precipitation, and it never appeared to cease. Mean flowering was 8.0 ± 0.5% by observation (n = 52). The GAM model indicated that greater flowering was correlated with hotter minimum temperatures (MINTc) and dry conditions, DroughtClass (R^2 = 18.7%, Appendix 3). Although drought flowering was significantly more than wet year flowering, both are extremely high. Neither photoperiodic nor insolation control of flowering was found and flowering never stopped during wet or dry years, summer or winter (Figure 5.10). This is the only species with no critical inflection points for light or precipitation.

DISCUSSION

Primary Abiotic Factors

Early in the data analysis, graphs made it clear that the flowering of most species was synchronized to the photoperiodic cycle, with several patterns identified. The first was flowering periodicity identical to photoperiod as in *M. polymorpha*. Second is flowering periodicity opposite to photoperiod as in *C. oppositifolia*. There are spring flowering-only or fall flowering-only species, as in *D. konaensisis* and *P. odorata*, respectively. Finally, some species never stopped flowering, for example, *S. paniculatum* and male *D. sandwicensis*. Once these patterns were recognized, each was called the classical photoperiodic type (*C. oppositifolia*, *N. breviflorum*, *P. odorata*, and *C. oppositifolia* SDP, female *D. sandwicensis*, *D. konaensisis*, *M. polymorpha*, and *P. sandwicensis* LDP, and male *D. sandwicensis* and *S. paniculatum* NDP).

The key to classifying these species into the PRT types was having multiyear, monthly phenological observations. Only the neutral-day species did not have one of the significant photoperiodic variables. The drought enabled us to separate the effects of precipitation and photoperiodism on flowering phenology. For 4 of the 10 species, multiyear drought only modified the amount but not the timing or duration of flowering. This strengthened the evidence for precipitation as a secondary factor at the study site, with photoperiodism the only primary abiotic factor controlling flowering periodicity. Greater precipitation only controlled the amount of flowering or, in some cases, delayed (one to two months) flowering.

The results found CDLs for four of eight species (1 SDP/3 LDP). The Ka'ūpūlehu results showed that when all SDP trees were considered, the mean CDL was ≤12.1 ± 0.04 h (n = 4). The SDP response group flowered for 10 months (August–May). Only June and July had no flowering. The mean CDL was higher for LDP species, >12.3 ± 0.2 h (n = 4). LDP species had a shorter seven-month flowering season (March–September), centered in the summer. The common break between SDP and LDP plants has been reported as ±12.0 h (e.g., Saito 1962, Pokorny 2024). The mean day length for the Ka'ūpūlehu species was slightly higher, 12.2 ± 0.1 h (n = 8). Estimating the day length for mature forests is difficult, so our methodology could be used to expand phenological studies in other regions. The availability of photoperiod and insolation estimates for Ka'ūpūlehu allowed them to be statistically tested for correlation to flowering. This information has not been available except for dark chamber studies (Garner and Allard 1920, NASA 2024, NOAA 2017).

Secondary Abiotic Factors

The effects of secondary factors on flowering are either long-term or short-term precipitation (drought vs. wet years), short-term (rain lag), or temperature. Precipitation was a significant driver for each secondary factor, including temperature extremes. Six species had greater flowering during the drought prior to 2004. They included all three photoperiodic response types (SDP *N. breviflorum* and *X. hawaiiensis*, LDP female *D. sandwicensis* and *P. sandwicensis*, and NDP male *D. sandwicensis* and *S. paniculatum*). Short-day (winter flowering) species flowering in drought conditions represented a paradox, they retained their usual photoperiod

response and did not need more favorable conditions for reproduction. Trees on Kaʻūpūlehu may utilize deep water sources for their metabolism when necessary. The many freshwater springs along the leeward coast indicate perched lens aquifers of available moisture for deep-rooted species (BWS 2024). LDP species like hot, dry conditions, so they may be more resilient to drought. Two species flowered more during wet years. *Dracaena konaensisis* and *C. oppositifolia* thrived in the dry, rocky habitat, but both waited to begin reproduction when wetter conditions returned. The remaining species, *M. polymorpha* and *P. odorata*, showed only a slight (few months) delay in flowering with increased precipitation.

Critical rain lag was the most prevalent short-term precipitation effect, which affected seven species. Five of these reacted positively to prior wet conditions (*C. oppositifolia*, *D. konaensisis P. odorata*, female and male *D. sandwicensis*), and all showed more flowering prior (42–147 days) to the observation. *P. odorata*'s response to rains was to delay flowering (as mentioned above). For both *D. sandwicensis* genders, more flowering when the drought broke in 2004 was the last of dry-year flowering, or more accurately, the last of the flowering, e.g., *N. breviflorum* and *P. sandwicensis* both stopped flowering after 2004. Their rain lags showed dry conditions prior (189–217 days) to flowering increased flowering.

To summarize, six species had greater drought-year flowering (both *D. sandwicensis* genders, *N. breviflorum*, *X. hawaiiensis*, *P. sandwicensis*, and *S. paniculatum*), two species had more wet-year flowering (*C. oppositifolia* and *D. konaensisis*), and two species showed little effect of precipitation, other than a slight delay in flowering (*M. polymorpha* and *P. odorata*). Five are drought-adapted species (*D. sandwicensis* genders, *N. breviflorum*, *P. sandwicensis*, and *X. hawaiiensis*), having no flowering in wet years. The sixth species (*S. paniculatum*) flowered more prolifically during drought years, but its wet-year flowering was equally high. The wet-year flowering species (*D. konaensisis* and *C. oppositifolia*) had little drought flowering and only flowered with wetter conditions.

Short-Day Plants

Most flowering of *C. oppositifolia* was in the winter, which is a relatively short season (October–February). NPH (2009) reports it is blooming year-round, but sporadically, with cultivated trees (perhaps irrigated?) in almost continuous flower. Rock (1913) describes the prime habitat for *C. oppositifolia* as the Kona area, just south of Kaʻūpūlehu north of Puʻu Waʻawaʻa Forest Reserve (Figure 1). Trees here were often 10 m tall and 30 cm in diameter in the late 1800s and 1900s. Little and Skolmen (1989) observed that this area was still *C. oppositifolia*'s prime habitat, which includes the protected Kaʻūpūlehu Dry Land Preserve and the Puʻu Waʻawaʻa Forest Reserve.

Nothocestrum breviflorum flowered year-round during dry conditions during the study. Wet-year flowering ceased during midsummer but continued the rest of the year. Rock (1913) found *N. breviflorum* flowering in January in Kaʻū (Figure 1). *Nothocestrum breviflorum* is important as a host for the endangered Blackburn's sphinx moth (*Manduca blackburni*), the larvae of which only feed on the leaves, stems, flowers, and buds of members of the Solanaceae family. *Nothocestrum breviflorum* is among the few suitable hosts of Blackburn's moth and larvae in the dry forests (CPC 2018). Recently, however, the moth has shifted its host to tree tobacco (*Nicotiana glauca*), an invasive plant and member of the Solanaceae family that is spreading across dry, arid landscapes of the archipelago. Blackburn's sphinx moth is an important pollinator of *N. breviflorum* (CPC 2018) and the moth's rarity probably contributes to *N. breviflorum*'s low reproduction rate and endangered status.

Psydrax odorata was the only indigenous species in the survey. *Psydrax odorata* major flowering occurred in the fall (August–January), and less flowering occurred during the rest of the year. Drought and wet year flowering are identical, except wet year flowering is delayed (one month). *Psydrax odorata* flowers sporadically and mainly in the winter according to NPH (2009), whereas the Pollinator Partnership (2020) lists it as blooming year-round. The Mālama Pua

(2020) reports blooming only in the fall and winter.

Most flowering of *X. hawaiiensis* occurred in the summer and fall (June–January). It is a drought-loving species with little flowering during spring's increasing photoperiods and wetter years. Rock (1913) observed it blooming in midsummer, with the timing varying according to locality and environment. Koebele (2020) stated that cultivated *X. hawaiiensis* may flower for longer than just the summer.

Long-Day Plants

Dracaena konaensisis only flowered in the spring and had more flowers during wet years, about three times dry year levels. Rock (1913) described its golden flowers as appearing in the early spring in drier regions, but under wetter conditions, there was a delay until the summer months. In the Hawai'i Volcanos National Park (HVNP) (Figure 1), the *D. konaensisis* population had 31% of the trees in flower during late summer (Abbott and Pratt 1996). This site receives much more precipitation than Ka'ūpūlehu and may be one of the wetter localities that Rock (1913) mentioned as having a delay until the summer. Litteeng-Rosenberger (2005) found that *D. konaensisis* flowered in late spring and that drought conditions delayed flowering, the opposite of what Rock (1913) described.

Metrosideros polymorpha in Hawai'i grows continuously from areas receiving annual precipitation <500 mm to those receiving >11,000 mm and at elevations from sea level to >2,400 m. Old *M. polymorpha* can be only a few centimeters tall in the cool, high-altitude bogs or grow as creepers, crawling along the boggy surface (Rock 1913, NPH 2009). In forest reserves on the Big Island's Hamakua coast, *M. polymorpha* can attain heights of 30 m and diameters over 1 m (Adee and Conrad 1990). *Metrosideros polymorpha* var. *polymorph* changes leaf morphology in response to environmental changes and elevation. In dry, low-elevation habitats, *M. polymorpha* generally has large, glabrous leaves with lower nitrogen content and mass per area. Varieties on wetter, high-elevation sites tend to have smaller, pubescent leaves with a greater nitrogen content and leaf mass. Fine hairs on the leaf undersurfaces help resist freezing and the leaves are generally smaller (Berlin et al. 2000). The thick glabrous leaves at lower elevations are leathery and help resist drought better.

In general, pubescent leaves are an adaption to high-elevation varieties. Several studies that reported on var. *polymorpha* flowering are available from the Big Island, including sites near Hawai'i Volcanos National Park, Keauhou Ranch, and Kilauea Forest Reserve and represented habitats from near sea level to the tree line with varied precipitation regimes, dry to wet (Ralph and Fancy 1994, Hart et al. 2011, Wolfe et al. 2017). These studies showed spring–summer flowering periodicity (May–June) including at higher elevations. On the Big Island and O'ahu from 1970 to 1971, Porter (1973) found extended spring to winter flowering, depending on variety and habitat at study sites that are mostly wet (1,300–3,000 mm) and elevations from 15 to >2,100 m. Trees at low-mid elevation sites were the first to flower in the year (March–April). Next and having the longest flowering period were trees at mid-high elevations (March–November). The low-high elevation variety of *M. polymorpha* var *polymorpha* growing at Ka'ūpūlehu flowered in the summer (June–July) but later at higher elevations (August–September). Berlin et al. (2000) also observed both winter and summer flowering at several high-elevation (1,567–2,128 m) sites in the montane cloud forests where precipitation was >5,000 mm. Glabrous forms flowered in the spring and summer (April–July) whereas pubescent forms in the winter (November–January). Berlin et al. (2000) commented on the paradox of *M. polymorpha* flowering in the winter when irradiance and temperature were at their lowest. Our findings suggested that precipitation might be involved in delaying var. *polymorpha* peak flowering by one-month during the spring and summer of wetter years. However, this could be a response to the cooling effect of precipitation rather than increased moisture (Figure 3*C*).

In the southern hemisphere, temperate zone species of New Zealand *M. excelsa* flower 2 weeks in the southern summer (December–January; Bylsma et al. 2014). Flowering onset is speculated to be initiated by decreasing fall

day lengths and the immature buds dormant over winter. In the spring the buds continue their development and seed in the spring and summer (Sreekantan et al. 2001). *Metrosideros excelsa* has leaf morphology similar to several forms of *M. polymorpha* but has both leaf forms, e.g., glabrous juvenile and pubescent mature leaves. High-altitude Hawai'i varieties exhibit one or the other, pubescent or glabrous leaves. This suggests that since the Hawai'i *M. polymorpha* originates in the southern hemisphere, some varieties demonstrate ancestral responses to cold (vernalization) and day length. Similar switches are reported for other LDP plants (Bernier and Périlleux 2005).

Pouteria sandwicensis was found to be loving with maximum flowering (March–September). The NPH (2009) lists it as summer blooming in the summer as does (https://www.wildflower.org/plants/result.php?id_plant=PLSA2).

Diospyros sandwicensis

Both male and female, *D. sandwicensis* trees were drought-loving at Ka'ūpūlehu, with females classified as summer flowering LDP plants and males as NDP. Females show flowering peaks in both wet and dry years from April to September. Males flowered year-round during dry years, but flowering was much reduced in wet years. Lamoureux (1973) found peak *D. sandwicensis* flowering spring and early summer in the HVNP. The Pollinator Partnership (2020) and Mālama Pua (2020) also list *D. sandwicensis* as blooming year-round. We found that males and females flower continuously during drought but not during wet years.

Neutral-Day Plants

Santalum paniculatum flowered continuously with slightly more flowering during the drought. It is a hemiparasite on root systems with suitable hosts including *S. paniculatum* are 'a'ali'i (*Dodonaea viscosa*), koa (*Acacia koa*), koai'a (*Acacia koaia*), māmaki (*Pipturus albidus*) 'ūlei (*Osteomeles anthyllidifolia*), ko'oko'olau (*Bidens asymmetrica*), naio (*Myoporum sandwicense*), and four of our study species, both *D. sandwicensis* genders, alahe'e, and 'ōhi'a (NPH 2009). Lamoureux's (1973) area observed that it flowers year-round in the Volcano area, with less flowering during winter. NPH (2009) indicates it flowers in the spring, summer, and fall and will not withstand waterlogging. This matches our findings of *S. paniculatum*'s aversion to precipitation. In the HVNP, 58% of the *S.* paniculatum were in flower in November/December (Abbott and Pratt 1996). The Pollinator Partnership (2020) lists it as blooming year-round. Mālama Pua (2020) lists *S. paniculatum* as blooming only in the summer.

There is no doubt from our results that photoperiodism is the major driver of flowering for these dry-land native species, not precipitation. For *M. polymorpha* on sites receiving over 5,000 mm annual precipitation, flowering is not concurrent with maximum precipitation (winter) but offset to the summer when biological activity should be lowest. It is only at higher elevations that the periodicity of flowering changes, most likely due to cold temperatures causing a slowing of tree metabolism. Insolation did not appear to be a major driver of flowering at Ka'ūpūlehu. Unlike nearer the equator, insolation does not have major summer fluctuations around the equinoxes.

The six drought-loving species may have advantages in surviving climate change, but only if they remain protected from invasive species and fire. Climate change predictions for Hawai'i are for dryer and hotter conditions, with reduced overland water flow (EPA 2016, 2024). The greatest impact may be through an increase in the frequency and intensity of the ENSO cycle. The drought from 1998 to 2003 was partly the consequence of an El Niño event.

ACKNOWLEDGMENTS

Climate Data: Nina Oakley, Assistant Research Climatologist, WRCC. Sylvia Mori, former PSW Station Mathematical Statistician. Special thanks to the field staff, Don Goo, Alan Murikami, Colleen Cole, and Roddy Nagata, all former IPIF Forestry Technicians. Thanks to two anonymous reviewers for their helpful suggestions and comments.

APPENDICES

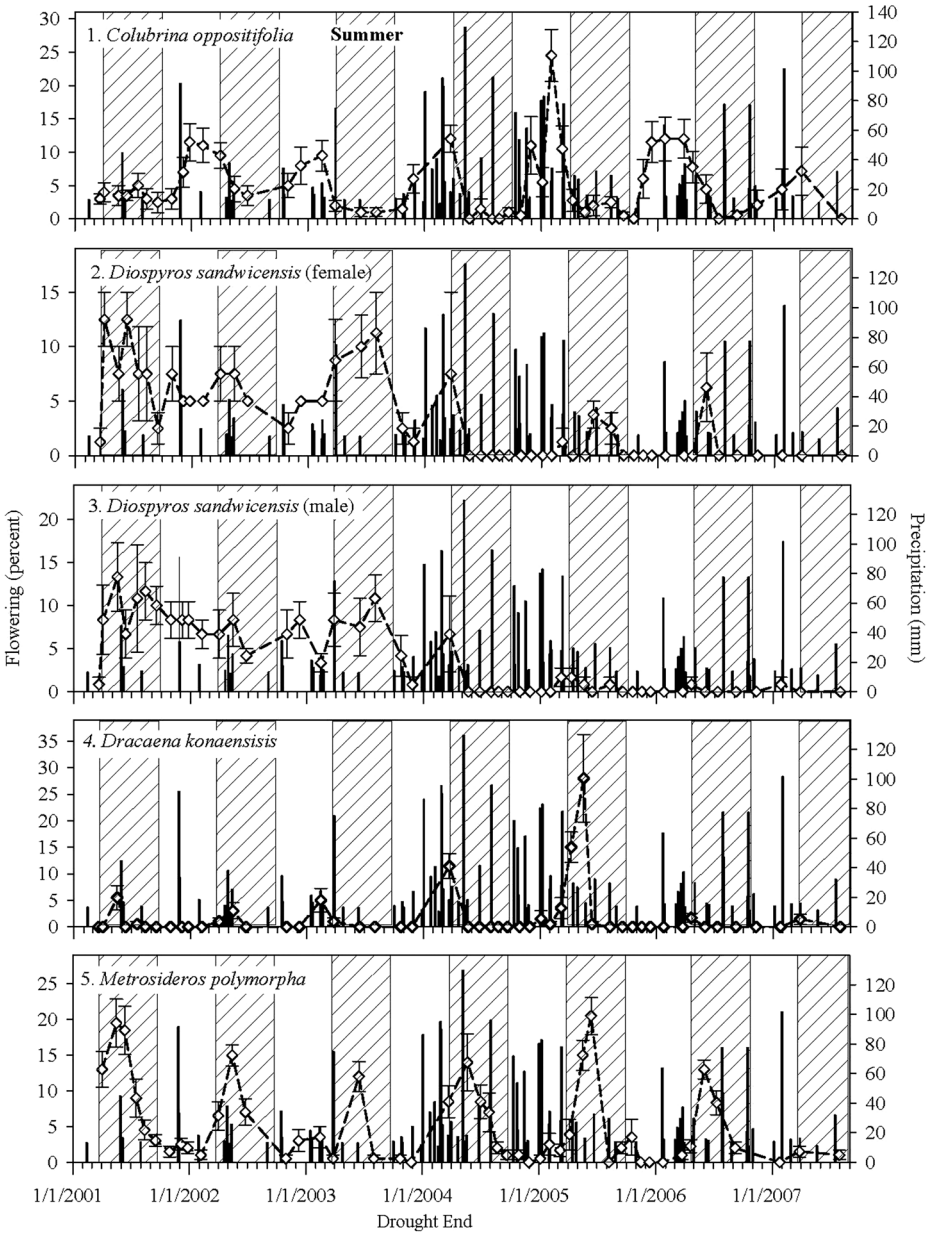

APPENDIX 1. Chronological dry land flowering species, by and measurement. Precipitation for entire study period shown on right *y*-axis. Symbols are: white diamonds = mean flowering, black vertical lines = precipitation. Error bars are 95% SE. Kaʻūpūlehu, Hawaiʻi, 2001–2007.

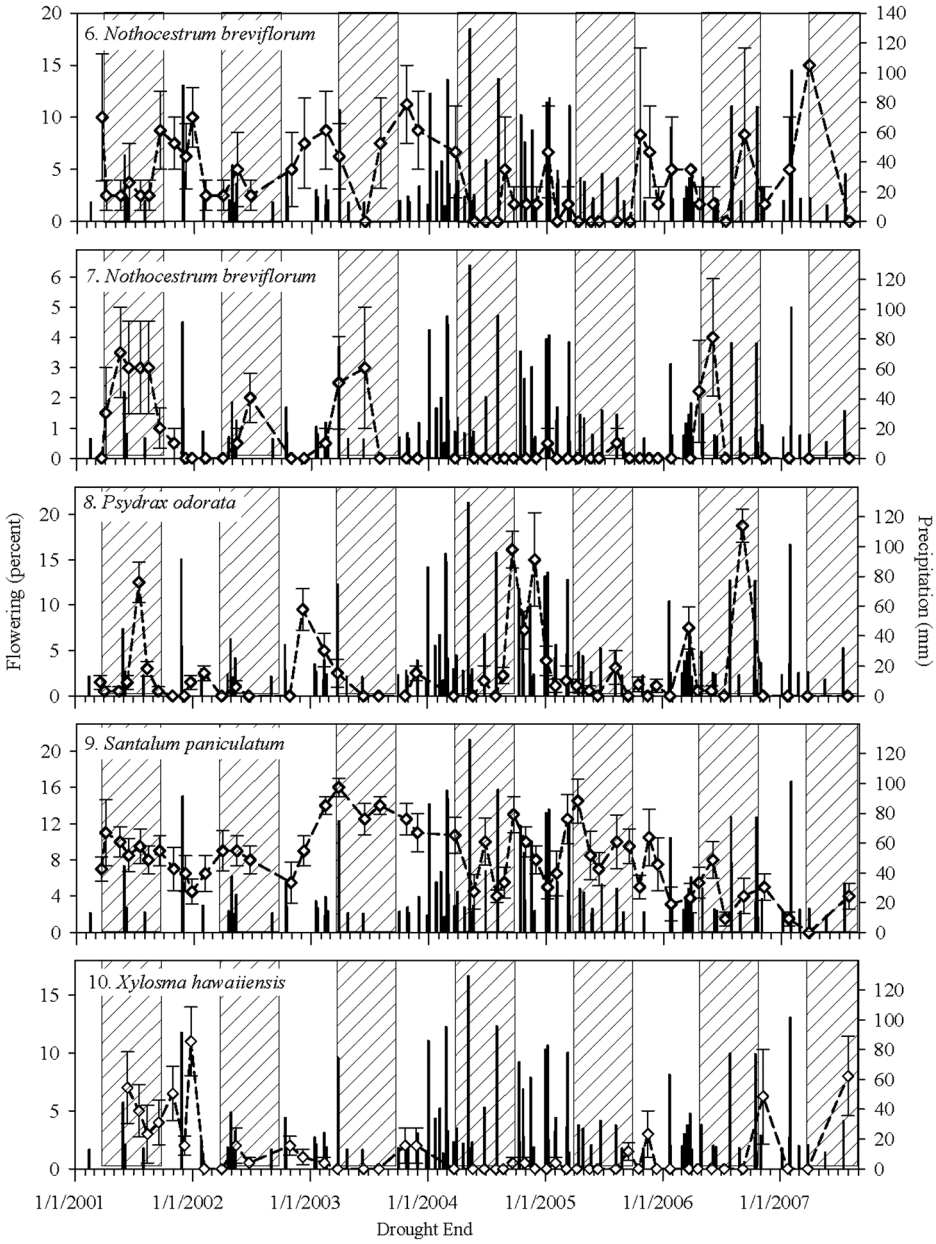

Appendix 1. (Continued).

Appendix 2. GAM libraries and GAM model code (R Core Team 2023). Ka‘ūpūlehu, Hawai‘i, 2001–2007.

1. #Load GAM libraries:
   a. library(mgcv) #mixed GAM w/Automatic Smoothness Estimation
   b. library(MASS)
   c. library(splines)
   d. library(openxlsx)
   e. library(nlme)
2. #Variables: mean flowering as dependent variable (2), independent biotic factors (8)
   a. MFLOWER = trees$MFLOWER
   b. lnMFLOWER = log(MFLOWER+1.0)
   c. PHOTOPER = trees$PHOTOPER
   d. INSOL = trees$INSOL
   e. AVETEMPC = trees$AVETEMPC
   f. MINTEMPC = trees$MINTEMPC
   g. MAXTEMPC = trees$MAXTEMPC
   h. $RAINLAG_{days}$ = $RAINLAG_{days}$ #days: 7, 14, 21 . . . 364 (52 variables)
   i. PRECIPCLASS = trees$PRECIPCLASS
   j. DROUGHTCLASS = trees$DROUGHTCLASS
   k. PHOTOCLASS = trees$PHOTOCLASS
3. #GAM models: model_1, or model_2 is ln transformation of flowering
   a. model_1<-gam(formula=MFLOWER~ DROUGHTCLASS + s(RAINLAG7), na.action = na.exclude, data=trees)
   b. model_2<-gam(formula=lnMFLOWER~DROUGHTCLASS + s(RAINLAG7), na.action = na.exclude, data=trees)
   c. summary(model_1)
   d. summary(model_2)
4. #Graph Residuals, change model_1 or model_2 (title to ln_mflower):
   a. pdf(“Species Name flower out.pdf”)
   b. par(mfrow=c(2,3),oma=c(0,2,0,2))
   c. for (i in 1:10) {
   d. lot(model_x,resid=F,all.terms=TRUE, select=i,scale=0)
   e. abline(h=0,col=“black”,lwd = 1)
   f. title(main = “MFLOWER”,cex.main=.7)
   g. }
   h. dev.off()

Appendix 3. General additive models (GAM) and statistics for dry land flowering species models. Codes are below.[1,2,3] Ka‘ūpūlehu, Hawai‘i, 2001–2007.

PRT Species	Model	Model (df)	Adj. R^2 (%)	r (%)	Parametric Coefficient	P
SDP						
C. oppositifolia	flower = PrC + $RLAG_{42}$	3	48.1	50.1	Intercept	$3.94e^{-9}$
					PrC	$7.17e^{-7}$
					$RLAG_{42}$	.0321
N. breviflorum	ln(flower) = s(PP) + s(INSOL) + s($RLAG_{189}$)	4	49.8	52.8	Intercept	$<2.00e^{-16}$
					s(PP)	.0004
					s($RLAG_{189}$)	$8.43e^{-6}$
					s(INSOL)	.0042
P. odorata	flower = PC + s($RLAG_{56}$)	3	15.6	19.8	Intercept	.0005
					PC	.0176
					s($RLAG_{56}$)	.0369

(table continues)

PRT Species	Model	Model (df)	Adj. R^2 (%)	r (%)	Parametric Coefficient	P
X. hawaiiensis	ln(flower) = PC + DC	3	23.6	26.8	Intercept	.6112
					PC	.0423
					DC	.0016
LDP						
D. sandwicensis (female)	ln(flower) = s(PP) + s($RLAG_{70}$) + DC	4	80.3	82.9	Intercept	$2.02e^{-7}$
					s(PP)	.0014
					s($RLAG_{70}$)	.0016
					DC	$2.22e^{-14}$
D. konaensisis	ln(flower) = PC + s($RLAG_{147}$)	3	48.9	52.3	Intercept	.0340
					PC	.0003
					s($RLAG_{147}$)	.0003
M. polymorpha	Flower = PC + s(PP) + s(INSO) + PrC	5	66.7	69.8	Intercept	.0078
					PC	$2.61e^{-6}$
					s(PP)	.0309
					s(INSOL)	.0153
					PrC	.0199
P. sandwicensis	ln(flower) = PC + s(PP) + s($RLAG_{217}$)	4	44.6	49.8	Intercept	.7895
					PC	.0349
					s(PP)	$5.46e^{-6}$
					s($RLAG_{217}$)	.0006
NDP						
D. sandwicensis (male)	ln(flower) = DC + s($RLAG_{91}$)	3	78.0	78.9	Intercept	$3.73e^{-10}$
					DC	$<2.00e^{-16}$
					s(RLAG91)	.0240
S. paniculatum	ln(flower) = DC + MINTC	3	18.7	21.9	Intercept	.8906
					MINTC	.0035
					DC	.0379

[1]Photoperiodic response types (PRT): short-day plants (SDP), long-day plants (LDP), or neutral-day plants (NDP).
[2]Coefficients: df, degrees freedom; PP, photoperiod; PC, PhotoClass, spring vs. fall photoperiods; INSOL, daily insolation; MINTC, minimum temperature; $RLAG_{DAYS}$, rain lag; PrC, PrecipClass, winter vs. summer seasons; and DroughtClass (DC), drought vs. wet years.
[3]Statistics: Adj. R^2, adjusted coefficient of determination; r, unadjusted coefficient of correlation; and probability (p). Transformations: ln, natural log and s, GAM spline.

Literature Cited

Abbott, L. L. and L. W. Pratt. 1996. Rare plants of Nāulu Forest and Poliokeawe Pali, Hawai'i Volcanoes National Park. Tech. Rpt. 108. USDI, USGS–BRD, PIERC, Hawai'i National Park Field Station. Univ. of Hawai'i.

Baker, H. G., and P. A. Cox. 1984. Further thoughts on dioecism and islands. Ann. Mo. Bot. Gard. 71:244–253.

Bernier, G., and C. Périlleux. 2005. A physiological overview of the genetics of flowering time control. Plant Biotechnol. J. 3:3–16.

Berlin K. E., T. K. Pratt, J. C. Simon, and J. R. Kowaisky. 2000. Plant phenology in a cloud forest on the island of Maui, Hawai'i. Biotrop. 32:90–99.

Borchert, R. 2024. The phenology of tropical trees. Online publication. Univ. Kansas. Accessed June 13, 2024. https://borchert.ku.edu/index.html.

Borchert, R., S. S. Renner, Z. Calle, D. Navarrete, A. Tye, L. Gautier, R. Spichiger, and P. von Hildebrand. 2005. Photoperiodic induction of synchronous flowering near the Equator. Nature 10:627–629. https://doi.org/10.1038/nature03259. PMID: 15703746.

Borchert, R. Z. Calle, A. H. Strahler, A. Baertschi, R. E. Magill, J. S. Broadhead, J. Kamau, J. Njoroge, and C. Muthuri. 2015. Insolation and photoperiodic control of tree development near the equator. New Phytol. 205:7–13. https://doi.org/10.1111/nph.12981.

BWS. 2024. Hawaii's water cycle. Board of Water Supply. Accessed https://www.boardofwatersupply.com/water-resources/oahu-water-history/the-water-cycle.

Bylsma, R. J., B. D. Clarkson, and J. T. Efford. 2014. Biological flora of New Zealand 14: *Metrosideros excelsa*, pōhutukawa, New Zealand Christmas tree. N. Z. J. Botany 52:365–385. https://doi.org/10.1080/0028825X.2014.926278.

Calle, Z., B. O. Schlumpberger, L. Piedrahita, A. Leftin, S. A. Hammer, A. Tye, and R. Borchert. 2010. Seasonal variation in daily insolation induces synchronous bud break and flowerings in the tropics. Trees 24:865–877. https://doi.org/10.1007/s00468-010-0456-3.

Cordell, S., and T. G Cole. 2024. Native tree phenology data from the Ka'ūpūlehu tropical dry forest, Hawai'i. Forest Service Research Data Archive, Fort Collins, CO. https://doi.org/10.2737/RDS-2024-0067.

Cordell, S., and D. R. Sandquist. 2008. The impact of an invasive African bunchgrass (*Pennisetum setaceum*) on water availability and productivity of canopy trees within a tropical dry forest in Hawai'i. Funct. Ecol. 22(6):1008–1017. https://doi.org/10.1111/j.1365-2435.2008.01471.x.

CPC. 2018. Plant profile *Nothocestrum breviflorum*. CPC National Collection Plant Profiles. Center for Plant Conservation. Accessed November 2020. https://saveplants.org/national-collection/plant-search/plant-profile/?CPCNum=2962.

DOFAW. 2019. 'Āhihi-Kīna'u Natural Area Reserve. Division of Forestry and Wildlife (DOFAW). Dept. Land and Natural Resources, State of Hawaii. pp. 2. Accessed July 3, 2024 https://dlnr.hawaii.gov/ecosystems/files/2019/08/Dryland-forest-Ahihi-Kinau.pdf.

Efron, B., and R. Tibshirani. 1991. Statistical data analysis in the computer age. Science 253:390–395.

EPA. 2016. What climate change means for Hawai'i. US Environmental Protection Agency (EPA 430-F-16-013). pp. 2. Accessed January 1, 2020 https://19january2017snapshot.epa.gov/sites/production/files/2016-09/documents/climate-change-hi.pdf.

———. 2024. El Nino and its impacts on Hawaii. Pacific ENSO Applications Climate (PEAC) Center. Accessed January 1, 2024 https://www.weather.gov/media/peac/one_pagers/El%20Nino%20Impacts%20on%20Hawaii.pdf.

Garner, W. W., and H. A. Allard. 1920. Effect of the relative length of day and night and other factors of the environment on growth and reproduction in plants. J. Agric. Res. 18:553–606.

Gaira, K. S., U. Dhar, and O. K. Belwal. 2011. Potential of herbarium records to sequence phenological pattern: a case study of *Acnitum heterophyllum* in the Himalaya. Biodivers. Conserv. 20:2210–2210.

Giambelluca, T. W., Q. Chen, A. G. Frazier, J. P. Price, Y. L. Chen, P. S. Chu, J. K. Eischeid, and D. M. Delparte. 2013. Online precipitation atlas of Hawai'i. Bull. Amer. Meteor. Soc. 94:313–316. https://doi.org/10.1175/BAMS-D-11-00228.1.

Hart, P. J., B. L. Woodworth, R. J. Camp, K. Turner, K. McClure, K. Goodall, C. Henneman, C. Spiegel, J. LeBrun, E. Tweed, and M. Samuel. 2011. Temporal variation in bird and resource abundance across an

elevational gradient in Hawaii. Auk. 128(1):113–126.
Hastie, T. J., and R. J. Tibshirani. 1986. Generalized additive models. Stat. Sci. 1(3): 297–318.
———. 1990. Generalized additive models. Chapman and Hall, London.
HFIA. 2017. Kaʻūpūlehu Restoration Project. Hawai'i Forest Industry Association (HFIA). ʻOʻōkala, Hawai'i. Accessed from: http://www.hawaiiforest.org/index.php/article/kaupulehu_restoration_project.
Hudson, I. L., A. Barnett, M. R. Keatley, and P. K. Ades, 2003. Investigation into drivers for flowering in Eucalyptus: Effects of Climate of Flowering. Pages 195–200 *in* G. Verbeke, G. Molenberghs, A. Aerts, andS. Fieuws, eds. Proceedings of the 18th international workshop on statistical modelling. Katholieke Universiteit Leuven, Leuven. http://www.statmod.org/files/proceedings/iwsm2003_proceedings.pdf.
Hudson, I. L., S. W. Kim, and M. R. Keatley, 2009. Climatic influences on the flowering phenology of four Eucalypts: a GAMLSS approach. Pages 2377–2383 *in* R. S. Andersen, R. D. Braddock, and L. T. H. Newham, eds. The proceedings of the 18th world IMACS congress and MODSIM09 international congress on modelling and simulation. Modelling and Simulation Society of Australia and New Zealand and International Association for Mathematics and Computers in Simulation, July 2009. ISBN: 978-0-9758400-7-8. http://www.mssanz.org.au/modsim09/F12/kragt.pdf.
Hui Mauli Ola. 2024. Ke ala o ka mahina (Moon Calendar). Accessed online January 1, 2018 https://www.huimauliola.org/.
Klebs, G. 1914. Über das Treiben der einheimischen Bäume, speziell der Buche. Abhandl. Heidelberger Akad. Wiss. (Math. Nat. Kl.) 3: 1–112. Translation in Borchert et al. 2015.
Koebele, B. 2020. A Native Hawaiian Garden. Accessed November 2020 http://www.nativehawaiiangarden.org/home.
Lamoureux, C. H. 1973. Phenology and growth of Hawaiian plants, a preliminary report. Islands Ecosystems IRP. US International Biological Program. Dept. Botany, Univ. Hawai'i, Honolulu, Hawai'i. Technical Report No. 24.
Lang, A. 1965. Physiology of flower initiation. Pages 1380–1536, Vol. XV, Part 1 *in* W. Ruhland, ed. Encyclopedia of plant physiology. Springer Verlag, Berlin.
Larsen, K. 2015. GAM: The Predictive Modeling Silver Bullet. San Francisco, CA. https://multithreaded.stitchfix.com/blog/2015/07/30/gam/.
Lawson, D. A., and S. A. Rands. 2019. The effects of rainfall on plant–pollinator interactors. Arthropod Plant Interact. 13: 261–569. https://doi.org/10.1007/s11829-019-09686-z.
Libby, R. 2018. Factors that affect natural regeneration, growth, and survival rates of threatened and endangered species in dryland forests of Hawai'i. A thesis submitted to the graduate division of the University of Hawai'i at Manoa in partial fulfillment of the requirements for the degree of master of science in botany, p. 60.
Litteeng-Rosenberger, K. E. 2005. Growing Hawai'i's native plants. Mutual Publishing LLC, Honolulu, HI.
Little, E. L., and R. G. Skolmen. 1989. Common Forest trees of Hawai'i (native and introduced). Agricultural Handbook No. 679. Forest Service, U.S. Department of Agriculture. Washington, DC.
Mālama Pua. 2020. Mālama Pua: Helping Univ. Hawai'i's pollinators. Online database. Accessed December 2020. CTAHR, Coop. Ext. Univ. Hawai'i. https://cms.ctahr.hawaii.edu/pollinators/.
Meeus, J. 1999. Astronomical algorithms. Willmann-Bell, Inc. Richmond, VA.
Moore, R. B., D. A. Claque, M. Rubin, and W. A. Bohrson. 1987. Hualalai-volcano: A preliminary summary of geologic, petrologic, and geophysical data. Chapter 20 in Volcanism in Hawai'i. Professional paper 1350, Pages 571–585. U.S. Geological Service. U.S. Gov. Printing Office, Washington, DC.
NASA. 2024. GISS: Insolation at specified location. Goddard Space Flight Center. Accessed December 12, 2024. https://data.giss.nasa.gov/modelE/ar5plots/srlocat.html.

NOAA. 2017. Sunrise/Sunset Calculator (Microsoft Excel). National Oceanic and Atmospheric Administration (NOAA), Earth System Research Laboratory, Global Monitoring Division, U.S. Department of Commerce. Boulder, Colorado. Accessed from http://www.esrl.noaa.gov/gmd/grad/solcalc/calcdetails.html.

NPH. 2009. Native Plants Hawai'i. Online Hawaiian native species database. Univ. Hawai'i. Accessed November 2020. http://nativeplants.hawaii.edu/plant/index.

Olson, S. L., and James, H. F. (1982). Fossil birds from the Hawai'ian Islands: evidence for wholesale extinction by man before western contact. Science 217(4560):633–635.

Phytosphere. 2001. Guidelines for developing and evaluating tree ordinances. http://phytosphere.com/treeord/treeord.pdf.

Pokorny, K. 2024. What are short-day and long-day plants? OSU Extension Service. Accessed January 26, 2025. https://news.oregonstate.edu/news/what-are-short-day-and-long-day-plants.

Polansky, L., and M. M. Robbins. 2013. Generalized additive mixed models for disentangling long-term trends, local anomalies, and seasonality in fruit tree phenology. Ecol. Evol. 3:3141–3151. https://doi.org/10.1002/ece3.707.

Pollinator Partnership. 2020. Selecting plants for pollinators in the ecological region of the Hawaiian Islands province. HI Dept. Ag. Regional Guide.

Porter, J. R. 1973. The growth and phenology of *Metrosideros* in Hawai'i. Tech Report No 27. Island Ecosystem, IRP, US Inter. Biol. Prog., Dept. Botany., Univ. Hawai'i.

R Core Team. 2023. R: A language and environment for statistical computing, version 4.4.0. R Foundation for Statistical Computing, Vienna, Austria. https://www.R-project.org/.

Ralph, C. J., and S. G. Fancy. 1994. Timing of breeding and molting in six species of Hawaiian honeycreepers. Condor 96:151–161.

Rivera, G., and R. Borchert. 2001. Induction of flowering in tropical trees by a 30-min reduction in photoperiod: evidence from field observations and herbarium specimens. Tree Physio. 21:201–212.

Rivera, G., S. Elliott, L. S. Caldas, G. Nicolossi, V. T. R. Coradin, and R. Borchert. 2002. Increasing day-length induces spring flushing of tropical dry forest trees in the absence of rain. Trees 16:445–456.

Roberts, A. M. I. 2008. Exploring relationships between phenological and weather data using Guillermo, R., S. Elliott, L. S. Caldas, G. Nicolossi, V. T. R. Coradin, and R. Borchert. 2002. Increasing day-length induces spring flushing of tropical dry forest trees in the absence of rain. Trees 14:445–456. https://doi.org/10.1007/s00468-002-0185-3.

Rock, J. F. 1913. Indigenous Trees of the Hawaiian Islands. Hawaiian Gazette Co., Ltd., Honolulu, T.H. (Territory of Hawai'i).

Saito, Y. 1962. Long-day and short-day tree species amongst *Coniferae*. Hokkaido Univ. Bulletin 21(2):373–376. Accessed from http://hdl.handle.net/2115/20804.

Sakai, A. K., W. L. Wagner, D. M. Ferguson, and D. R. Herbst. 1995. Origins of dioecy in the Hawaiian flora. Ecol. 76:2517–2529.

Sreekantan, L., M. J. McKenzie, P. E. Jameson, and J. Clemens. 2001. Cycles of floral and vegetative development in *Metrosideros excelsa* (Myrtaceae). Int. J. Plant Sci. 162:719–727.

Steel, R. G. D., and J. H. Torrie. 1980. Principles and procedures of statistics: a biometrical approach. 2nd ed. McGraw-Hill Book Company, Inc., New York, NY.

Stiles, F. G. 1978. Temporal organization of flowering among the hummingbird food plants of a tropical wet forest. Biotropica 10:194–210.

Thuma, J. A., C. Duff, M. Pitera, N. Januario, C. M. Orians, and P. T. Starks. 2023. Nutrient enrichment and rainfall affect plant phenology and floral resource availability for pollinators. Front. Ecol. Evol. 11:1150736. https://doi.org/10.3389/fevo.2023.1150736.

USFWS. 2020*a*. Threatened and Endangered Species Active Critical Habitat Report. ECOS Environmental Conservation Online System. U.S. Fish Wildlife Service, Department of Interior. Accessed November 2020. https://ecos.fws.gov/ecp/report/critical-habitat.

———. 2020*b*. USFSW Species Data Explorer. ECOS Environmental Conservation Online System. U.S. Fish Wildlife Service, Department of Interior. Accessed November 2020. https://ecos.fws.gov/ecp/report/adhoc-creator?catalogId=speciesandreportId=speciesandcolumns=%2Fspecies@cn,sn,status,desc,listing_dateandsort=%2Fspecies@cn%20asc;%2Fspecies@sn%20asc.

Uzoh, F. C. C., and S. R. Mori. 2012. Applying survival analysis to managed even-aged stands of ponderosa pine for assessment of tree mortality in the western United States. For. Ecol. Mang. 285: 101–122.

Wada, K. 2003. Physiology of flowering in *Pharbitis nil*. Niigata University. Flowering terminology. https://www.sc.niigata-u.ac.jp/biologyindex/wada/english/index2.html.

Wagner, W. L., D. R. Herbst, and S. H. Sohmer. 1990. Manual of the flowering plants of Hawai'i. 2 vols., Bishop Museum Special Publication 83. University of Hawai'i Press and Bishop Museum Press, Honolulu.

———. 1999. Manual of the flowering plants of Hawai'i. Revised edition. Univ. Hawai'i Press, Bishop Museum Press. Honolulu, Hawai'i.

Wolf, J. D., C. J. Ralph, and A. Wiegardt. 2017. Bottom-up processes influence the demography and life–cycle phenology of Hawaiian bird communities. Ecol. 98: 2885–2894.

Wood, S. N. 2006. Generalized additive models: an introduction with R. Chapman and Hall/CRC. New York, NY.

———. 2011. Fast stable restricted maximum likelihood and marginal likelihood estimation of semiparametric generalized linear models. J. R. Stat. Soc. 73:3–36.

———. 2023. Package 'mgcv'. Online R GAM package documentation. https://cran.r-project.org/web/packages/mgcv/index.html https://doi.org/10.1201/9781315370279.

WRCC. 2012. Cooperative climatological data summaries: Kona International Airport (2000–2012). Data supplied upon request from the Western Regional Climate Center (WRCC), Desert Research Institute, Reno, NV.

Yeang H.-Y. 2007*a*. Synchronous flowering of the rubber tree (*Hevea brasiliensis*) induced by high solar intensity. New Phytol. 175:283–289.

———. 2007*b*. The sunshine-mediated trigger of synchronous flowering in the tropics: the rubber tree as a study model. New Phytol. 176:730–735.